NUMERICAL SIMULATION OF BURGERS FLOW BY WAVELET METHOD

D.Černá, V. Finěk

Department of Mathematics and Didactics of Mathematics, Technical University in Liberec

Abstract

The paper is concerned with a numerical simulation of Burgers flow as a simplified model of unsteady flow of a compressible viscous fluid. Viscous Burgers equation represents many of the properties of unsteady compressible Navier-Stokes equations, such as nonlinear convection and viscous diffusion leading to shock waves and boundary layers. A one-dimensional Burgers equation is frequently used to test new methods because an analytic solutions are known for different boundary and initial conditions.

We follow some ideas from [1, 3, 5], where a general wavelet adaptive method for a large class of nonlinear equations has been proposed and we solve Burgers equation by a wavelet adaptive method. The adaptivity in the context of wavelet discretization insists in establishing which wavelet coefficients to keep and which to discard. The specific difficulty is that the singularities might move in time and so the set of indices of significant wavelet coefficients at each time step should be updated. The computational complexity for all steps of our algorithm is controlled. The computation is carried out in MATLAB using a PDE Toolbox and Wavelet Toolbox.

1 Motivation - compression property of wavelets

Let us approximate the function f by a combination

$$f_N = \sum_{(j,k)\in J_N} c_{j,k}\psi_{j,k},$$

where $\#J_N = N$ and $\psi_{j,k}$ are suitable wavelets. A function f that is smooth, except at some isolated singularities, typically has a *sparse representation* in a wavelet basis, i.e. only a small number of numerically significant coefficients carry most of the information on f. Figure 1 displays a function f sampled on 2^9 points and its reconstruction from 50 largest wavelet coefficients. Wavelets used for decomposition are Daubechies wavelets with two vanishing moments. The largest coefficients are also displayed in Figure 1, the x-axis represents the center of the support of wavelet corresponding to given coefficient and y-axis represents the level of resolution (j). The function f has sharp derivative at the point $x = 0.5$ and so we can observe that the approximation is automatically refined near this point. This *compression property* of wavelets has many applications. Most important are data compression, signal analysis, and efficient adaptive schemes for PDE's.

Figure 1:

function f | 50 significant coefficients | approximation f_N of f

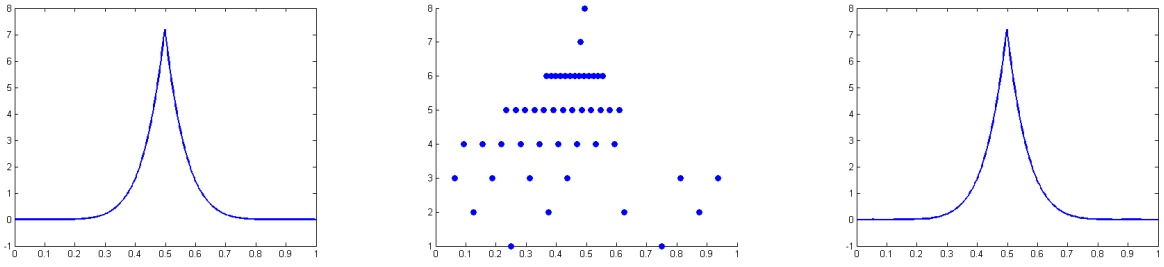

2 Viscous Burgers equation

Let $\Omega = \langle a, b\rangle$ be a bounded interval, $T > 0$ and $Q_T := \Omega \times (0, T)$. We consider viscous Burgers equation with homogeneous Dirichlet boundary conditions: Find $u : Q_T \to \mathbb{R}$ such that

$$\frac{\partial u}{\partial t} + u\frac{\partial u}{\partial x} = \nu\frac{\partial^2 u}{\partial x^2} \qquad \text{in} \qquad Q_T \tag{1}$$

with initial and boundary conditions

$$u\,(x, 0) = u^0\,(x) \quad \text{for } x \in \Omega \qquad \text{and} \qquad u\,(a, t) = u\,(b, t) = 0 \quad \text{for } t \in (0, T). \tag{2}$$

We assume that $\nu > 0$, $u^0 \in L^2\,(\Omega)$. We also consider Burgers equation with periodic boundary conditions.

Burgers equation is derived from the Navier-Stokes equation in the case of a one-dimensional non-stationary flow of a compressible viscous fluid and it models a flow through a shock wave. This equation is frequently used to test new methods because an analytic solutions are known for different boundary and initial conditions and because for small values of ν solutions typically develop very sharp gradients which are difficult to reproduce with numerical methods.

Weak solution of viscous Burgers equation is defined as a function u satisfying:

1) $u \in L^2\left(0, T; H_0^1\,(\Omega)\right), \quad u \in L^\infty\,(Q_T)\,,$

2) $\dfrac{\mathrm{d}}{\mathrm{d}t}\,\langle u\,(t)\,, v\rangle + \displaystyle\int_\Omega u\frac{\partial u}{\partial x}v\mathrm{d}x + \nu\int_\Omega \frac{\partial u}{\partial x}\frac{\partial v}{\partial x}\mathrm{d}x = 0 \quad \text{for all} \quad v \in H_0^1\,(\Omega)\,,$

3) $u\,(0) = u^0 \quad \text{in} \quad \Omega.$

The symbol $\langle\cdot,\cdot\rangle$ denotes standard $L^2\,(\Omega)$ product. $H_0^1\,(\Omega)$ denotes the subspace of all functions from $H^1\,(\Omega)$ with zero traces on $\partial\Omega$, $H_0^{-1}\,(\Omega)$ denotes its dual. It is known that there exists a unique weak solution and it satisfies $\dfrac{\partial u}{\partial t} \in L^2\,(Q_T)$. Periodic boundary conditions are treated in a similar way.

3 Discretization

Let $h > 0$, $t_k := kh$ and u^k be an approximation of $u\,(\cdot, t_k)$. We use following explicit methods for discretization in time:

Forward Euler method (FE)

$$\frac{u^{k+1} - u^k}{h} + u^k\frac{\partial u^k}{\partial x} = \nu\frac{\partial^2 u^k}{\partial x^2} \tag{3}$$

Adams-Bashforth method (AB)

$$\frac{u^{k+1} - u^k}{h} + \frac{3}{2}u^k\frac{\partial u^k}{\partial x} - \frac{1}{2}u^{k-1}\frac{\partial u^{k-1}}{\partial x} = \frac{3}{2}\nu\frac{\partial^2 u^k}{\partial x^2} - \frac{1}{2}\nu\frac{\partial^2 u^{k-1}}{\partial x^2} \tag{4}$$

Euler-Adams-Bashforth method (EAB)

$$\frac{u^{k+1} - u^k}{h} + \frac{3}{2}u^k\frac{\partial u^k}{\partial x} - \frac{1}{2}u^{k-1}\frac{\partial u^{k-1}}{\partial x} = \nu\frac{\partial^2 u^k}{\partial x^2} \tag{5}$$

While forward Euler method is first order accurate with respect to the time-step h, Adams-Bashforth method is second order accurate. The error for Euler-Adams-Bashforth method is almost the same as the error for Adams-Bashforth method, see Example 1. and Example 2. below. Since AB and EAB are two-step methods, they are slightly slower than FE. It is known these explicit schemes are not unconditionally stable, i.e. stability depends on the size of time step and number of basis functions used for spatial discretization. Time steps giving stability for different time discretizations are shown in Table 1.

We use Petrov-Galerkin method for discretization in space. Basis and test functions will be wavelets adapted to the interval and boundary conditions. In this case the problem reads:

$$\text{Find} \quad u_n^{k+1} \in V_n^{k+1} \quad \text{such that} \quad a_k\left(u_n^{k+1}, v\right) = f^k(v), \quad \text{for all} \quad v \in \tilde{V}_n^{k+1}, \tag{6}$$

where $V_n^k, \tilde{V}_n^k \subset H_0^1(\Omega)$, $\dim V_n^k = \dim \tilde{V}_n^k < +\infty$, $V_n^k \subset V_{n+1}^k$, $\tilde{V}_n^k \subset \tilde{V}_{n+1}^k$ and $\overline{\bigcup_{n\in\mathbb{N}} V_n^k} = \overline{\bigcup_{n\in\mathbb{N}} \tilde{V}_n^k} = H_0^1(\Omega)$. A continuous bilinear form $a_k : H_0^1(\Omega) \times H_0^1(\Omega) \to \mathbb{R}$ and $f^k \in H_0^{-1}(\Omega)$ are defined by the standard way.

Let $\{\psi_\lambda, \lambda \in J\}$ be a basis of V_n^k, $\left\{\tilde{\psi}_\lambda, \lambda \in J\right\}$ be a basis of $\tilde{V}_n^k$ (for the sake of simplicity we omit indexes k and n). Let d_λ^k be such that $u_n^{k+1} = \sum_{\lambda\in J} d_\lambda^{k+1}\psi_\lambda$. Then algebraic formulation of our problem reads:

$$\mathrm{M}^k \mathrm{d}^{k+1} = \mathrm{f}^k,$$

where $\mathrm{M}_{i,j}^k = a_k(\psi_i, \tilde{\psi}_j)$, $\mathrm{f}_i^k = \left\langle f^k, \tilde{\psi}_i \right\rangle$ and $\mathrm{d}_i^{k+1} = d_i^{k+1}$. In the sequel we assume that $\{\psi_\lambda, \lambda \in J\}$ and $\left\{\tilde{\psi}_\lambda, \lambda \in J\right\}$ are biorthogonal wavelet bases.

Definition 1. Family $\Psi := \{\psi_\lambda, \lambda = (j,k) \in J\}$ for infinite set $J = J_\phi \cup J_\psi$, $\#J_\phi < \infty$, is called *wavelet basis* of $V \subset H^s(\Omega)$, if

1) Ψ is a *Riesz basis* of V, that means Ψ generates V and there exist constants $c, C \in (0,\infty)$ such that for all $\mathrm{b} := \{b_\lambda\}_{\lambda\in J} \in l^2(J)$, where $|\lambda| := j$ for $\lambda := (j,k)$ holds

$$c\,\|\mathrm{b}\|_{l_2(J)} \le \left\| \sum_{\lambda\in J} b_\lambda 2^{-s|\lambda|}\psi_\lambda \right\|_{H^s(\Omega)} \le C\,\|\mathrm{b}\|_{l_2(J)}.$$

2) Functions are *local* in the sense that $\operatorname{diam}(\Omega_\lambda) \le \mathrm{C}2^{-|\lambda|}$ for all $\lambda \in J$, where Ω_λ is support of ψ_λ.

3) Functions have *cancellation properties* of order m, i.e.

$$|\langle v, \psi_\lambda\rangle| \le C2^{-m|\lambda|}\,|v|_{H^m(\Omega_\lambda)}, \quad \lambda \in J_\psi, \quad v \in V.$$

There exists a biorthogonal wavelet basis $\tilde{\Psi}$ to any wavelet basis Ψ, that means a basis satisfying *i*), *ii*) and cancellation property *iii*) of order $\tilde{m}$. Any function $v \in V$ can be written in the form $v = \sum_{\lambda\in J} d_\lambda\psi_\lambda$, where $d_\lambda = \left\langle v, \tilde{\psi}_\lambda \right\rangle$.

We use *B-spline wavelet basis*, i.e. wavelet basis derived from B-spline wavelet designed in [2], which were adapted to the interval by periodization [7] (well-suited only for periodic problems) or treating boundary wavelets separately [6]. 1D wavelet basis constructed from quadratic B-spline adapted to homogeneous Dirichlet boundary condition is displayed in Figure 2 and Figure 3. Wavelet basis can be transformed to so called *scaling basis* by *discrete wavelet transform* (DWT) in $O(N)$ operations, where N is the number of basis functions. Riesz basis

property ensures stability of DWT. Scaling basis corresponds to nodal basis on uniform mesh while wavelet basis corresponds to hierarchical basis in the finite element theory and are used in the adaptive scheme. In all examples FE is combined with linear basis functions and AB, EAB are used with quadratic basis functions.

Figure 2: Scaling functions at the level 4

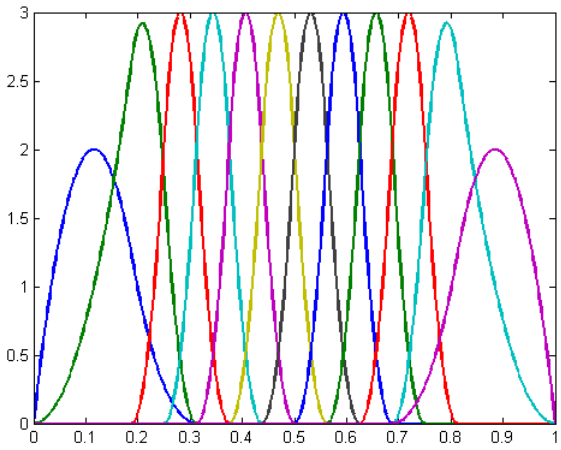

Figure 3: Wavelet functions at the level 4 and 5

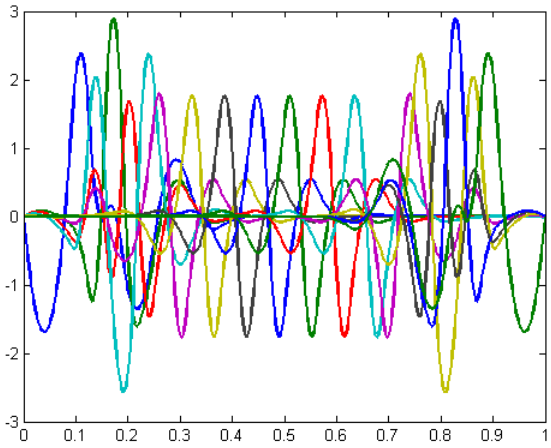

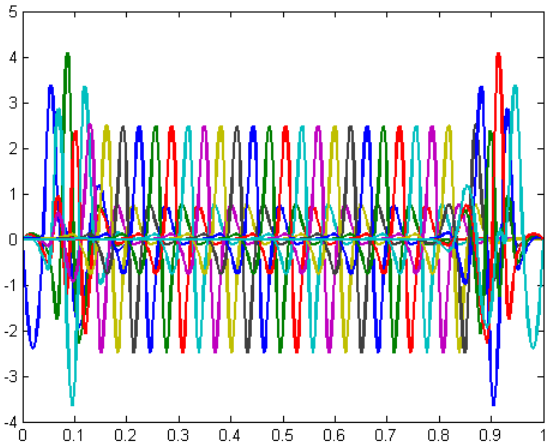

Let us define approximation of function u^{k+1} by:

$$u_n^{k+1} = \sum_{\lambda \in J_n} d_\lambda^{k+1} \psi_\lambda, \tag{7}$$

where $\#J_n = n$ and J_n contains indices of n largest values $\|d_\lambda \psi_\lambda\|$. This approximation is *near optimal* in the sense:

$$\left\| u^{k+1} - u_n^{k+1} \right\|_{H^p(\Omega)} \leq C \, \inf_{v \in S_n} \left\| u^{k+1} - v \right\|_{H^p(\Omega)}, \qquad 0 \leq p \leq s, \tag{8}$$

where $S_n = span\left\{\psi_\lambda, \lambda \in \Lambda, \#\Lambda \leq n\right\}$. And for $\dfrac{1}{q} = \dfrac{1}{p} + \dfrac{t}{d}$ it holds:

$$u^{k+1} \in W^{s+t,q} \Rightarrow \inf_{v \in S_n} \left\| u^{k+1} - v \right\|_{W^{s,p}} \leq C N^{-t/d}. \tag{9}$$

Now our aim is to design a scheme that in the above tracks sense the significant coefficients of u^{k+1}.

4 Adaptive numerical scheme

The algorithm has the following form

1) **Initialization** Compute wavelet coefficients $\left\{d_\lambda^0, \lambda \in J^0\right\}$ of u_0 given by initial condition.

2) **Iteration** We have index set J^k and wavelet coefficients d_λ^k, $\lambda \in J^k$, of u^k. Then we compute J^{k+1} and wavelet coefficients of u^{k+1} in these steps:

   i) *Refinement:* A set $\tilde{J}^{k+1} \supset J^k$ is derived from aposteriori analysis of wavelet coefficients.

   ii) *Solution:* By adaptive approximation of operators f^k, M^k we find solution of $\mathrm{M}^k \mathrm{d}^{k+1} = \mathrm{f}^k$ for $\mathrm{d}^{k+1} = \left\{d_\lambda^{k+1}, \lambda \in \tilde{J}^{k+1}\right\}$.

   iii) *Coarsening:* consists in thresholding wavelet coefficients d_λ^{k+1}. Index set $J^{k+1} \subset \tilde{J}^{k+1}$ corresponds to the largest coefficients. We can perform the coarsening only in every l-th step or we need not perform coarsening at all in the case that the singularity doesn't move.

5 Refinement strategies

At the k-th step we have a set of indices J^k. In order to track singularities we also keep *the adjacent coefficients* and if $2^{dm}\eta_{|\lambda|} \leq |d_\lambda| \leq 2^{d(m+1)}\eta_{|\lambda|}$ then we refine m levels above λ. Level dependent threshold $\eta_{|\lambda|}$ must be set appropriately to control the error of approximation. In our case we use $\eta_{|\lambda|} = 2^{d|\lambda|}\eta$ because this approach is appropriate for controlling the error in H^1 norm. On Figure 4 the set J_k is represented by blue points and the brown points are adjacent.

In the case of a traveling wave, see Example 2, the steep front can move too fast to be tracked with the scheme above. For this reason we further improve our strategy: We compare the largest wavelet coefficients on the same level of the last two index sets J^k and J^{k-1} and this gives us an information about the speed of the wave. For example, if the speed is two points to the right, we further refine two points to the right at every level, see the yellow points on Figure 4. And thus we obtain the new index set $\tilde{J}^{k+1}$.

Figure 4:

The set J_k and the adjacent points

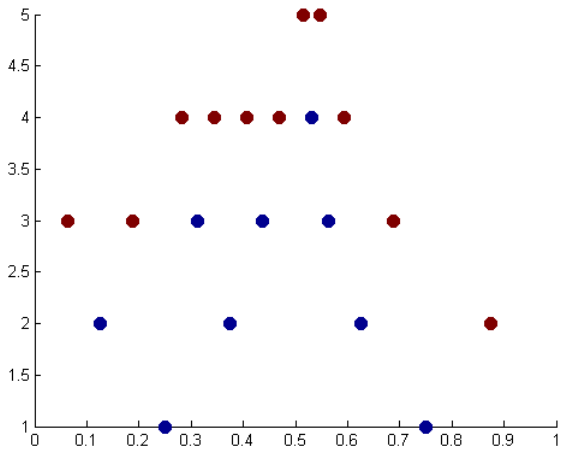

The set $\tilde{J}_{k+1}$

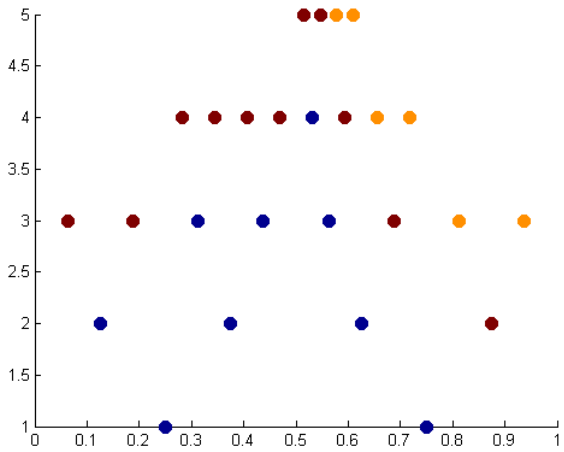

6 Numerical examples

Example 1. First we consider the solution with steep front on a stationary wave. Let us consider equation (1) for $\Omega = (0,1)$ with periodic boundary conditions

$$u(0,t) = u(1,t), \quad t \in (0,T) \tag{10}$$

and initial condition

$$u(x,0) = sin(2\pi x), \quad x \in (0,1). \tag{11}$$

Analytic solution of this task is given by

$$u(x,t) = \frac{\int_{-\infty}^{\infty} \frac{x-\xi}{t} \exp\left[-\frac{(x-\xi)^2}{4\nu t}\right] \exp\left[\frac{\cos(2\pi\xi)}{4\pi\nu}\right] d\xi}{\int_{-\infty}^{\infty} \exp\left[-\frac{(x-\xi)^2}{4\nu t}\right] \exp\left[\frac{\cos(2\pi\xi)}{4\pi\nu}\right] d\xi}.$$

This function develops a steep gradient at $x = 0.5$, which reaches a maximum of approximately 40.1 at $t = 0.27$. Accuracy results at $t = 0.27$ are given in Table 2. We can see that the forward Euler method approximates the gradient very badly and that the H^1 seminorm of the error is too large. Adaptive wavelet schemes are much more efficient than non-adaptive schemes with respect to number of degrees of freedom (dof) and computational work. Since the used algorithms are not unconditionally stable, we summarize in Table 1. numerically found sizes of the largest time-steps which ensure stability. Our aim was to obtain an idea of the stability region rather than to determine it accurately.

Figure 5: Solution of 1D Burgers equation - stationary wave

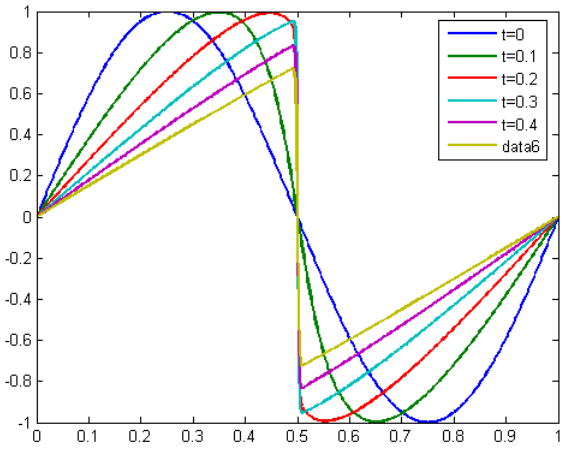

Table 1: Stability results for $\nu = 0.01$

Forward Euler method	Adams-Bashforth method	Euler-Adams-Bashforth method
64 dof Δt=0.002	64 dof Δt=0.002	64 dof Δt=0.004
128 dof Δt=0.0008	128 dof Δt=0.0005	128 dof Δt=0.001
256 dof Δt=0.0002	256 dof Δt=0.0001	256 dof Δt=0.0002

Table 2: Accuracy results of Burgers equation with conditions (10), (11), $\nu = 0.01$, and $t = 0.27$

method	Δt	basis functions	dof	uniform or adapt. or adapt.	L^∞ norm of error $\times 10^{-4}$	L^2 norm of error $\times 10^{-4}$	H^1 seminorm of error $\times 10^{-4}$	gradient at $x = 0.5$
FE	$5\ 10^{-4}$	linear	128	uniform	91	12	6355	38.6
FE	10^{-4}	linear	256	uniform	32	6	3183	39.8
AB	$5\ 10^{-4}$	quadratic	128	uniform	84	12	916	40.6
AB	10^{-4}	quadratic	256	uniform	39	6	484	40.2
EAB	$5\ 10^{-4}$	quadratic	128	uniform	83	12	912	40.6
EAB	10^{-4}	quadratic	256	uniform	39	6	483	40.2
FE	10^{-4}	linear	42	adaptive	35	10	3354	39.7
AB	10^{-4}	quadratic	40	adaptive	43	10	499	40.2
EAB	10^{-4}	quadratic	40	adaptive	42	10	498	40.2

Example 2. We have a situation of fast moving wave which develops a steep front. Let us consider equation (1) with homogeneous Dirichlet boundary conditions

$$u(0,t) = u(1,t) = 0 \tag{12}$$

and initial condition

$$u(x,0) = \frac{x}{1 + [\exp(1/8\nu)]^{-1/2} \exp(x^2/4\nu)}. \tag{13}$$

Analytic solution of this task is known and numerical results are presented in Table 2. Wavelet bases derived from B-splines were constructed as in [6].

Figure 6: Solution of 1D Burgers equation - traveling wave

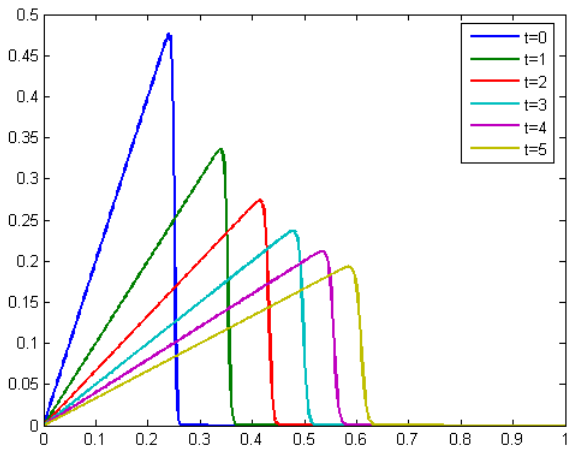

Table 3: Accuracy results of Burgers equation with conditions (12), (13) and $\nu = 0.001$, and $t = 0.7$

method	Δt	basis functions	dof	uniform or adapt.	L^∞ norm error $\times 10^{-4}$	L^2 norm error $\times 10^{-4}$	H^1 seminorm error $\times 10^{-4}$
FE	10^{-4}	linear	255	uniform	9	3	169
AB	10^{-4}	quadratic	252	uniform	4	1	38
EAB	10^{-4}	quadratic	252	uniform	4	1	39
FE	10^{-4}	linear	47 to 50	adaptive	10	4	170
AB	10^{-4}	quadratic	43 to 48	adaptive	5	1	40
EAB	10^{-4}	quadratic	43 to 48	adaptive	5	1	41

Acknowledgements. The first author is supported by research project 1M06047 financed by Ministry of Education, Youth and Sports of the Czech Republic, the second author is supported by research project LC06024 financed by Ministry of Education, Youth and Sports of the Czech Republic. Authors acknowledge this support.

References

[1] Cohen, A.: *Numerical Analysis of Wavelet Methods*, Elsevier Science, Amsterdam, 2003.

[2] Cohen, A.; Daubechies, I.; Feauveau, J.-C.: *Biorthogonal bases of compactly supported wavelets.* Comm. Pure and Appl. Math. 45: 485-560, 1992.

[3] Cohen, A.; Dahmen, V.; DeVore, R.: *Adaptive wavelet techniques in numerical simulation.* Encyclopedia of Computational Mathematics 1: 157-197, 2004.

[4] Cohen,A.; Dahmen, W.; DeVore, R.: *Adaptive wavelet methods II - Beyond the elliptic case.* Foundations of Computational Mathematics 2: 203-245, 2002.

[5] Dahmen, W.: *Multiscale and wavelet methods for operator equations.* Lecture Notes in Mathematics 1825: 31-96, 2003.

[6] Dahmen, W.; Kunoth, A.; Urban, K.: *Biorthogonal spline wavelets on the interval - stability and moment conditions.* Appl. Comp. Harm. Anal. 6: 132-196, 1999.

[7] Meyer, Y.: *Ondelettes et opérateurs 1-3: Ondelettes.* Hermann, Paris, 1990.

Dana Černá
Department of Mathematics and Didactics of Mathematics
Technical University in Liberec
Hálkova 6
Liberec 461 16, Czech Republic
dana.cerna@vslib.cz

Václav Finěk
Department of Mathematics and Didactics of Mathematics
Technical University in Liberec
Hálkova 6
Liberec 461 16, Czech Republic
vaclav.finek@vslib.cz